

# Shape suitability and mechanical safety of customised hip implants: Three-dimensional printed acetabular cup for hip arthroplasty

Yeokyung Kang<sup>a,b</sup>, Doo-Hoon Sun<sup>a,c</sup>, Jong-Chul Park<sup>b,\*\*</sup>, Jungsung Kim<sup>a,\*</sup>

<sup>a</sup> Central Research & Development Center, Corentec Company Ltd., 33-2, Banpo-daero 20-gil, Seocho-gu, Seoul, Republic of Korea

<sup>b</sup> Cellbiocontrol Laboratory, Department of Medical Engineering, Yonsei University College of Medicine, 50-1 Yonsei-ro, Sinchon-dong, Seodaemun-gu, Seoul, Republic of Korea

<sup>c</sup> Department of Orthopaedic Surgery, Daejeon Sun Hospital, 10-7 Mok-dong, Jung-gu, Daejeon, Republic of Korea

## ARTICLE INFO

### Keywords:

Customised implant  
Paprosky classification  
Mechanical performance  
Shape suitability  
Mechanical safety

## ABSTRACT

**Background:** Owing to an increase in the number of hip arthroplasty surgeries, the number of implant replacement surgeries is increasing rapidly as well. This necessitates the study of hip joint conditions. Therefore, Paprosky defined a classification system to indicate the degree of damage to the hip joint. In this study, a customised hip implant suitable for Paprosky classification Type IIC and over was designed. The shape, suitability, and mechanical safety of the worst-case model for the implant were evaluated.

**Materials and methods:** To identify the implant size depending on states over Type IIC acetabulum bone loss, a size range was selected and a customised implant was designed according to the computed tomography data within the size range. The implant was designed for the flange, hook, and flattened model types. The worst-case selection test was conducted using finite element analysis. The von Mises stresses of the flange, hook, and flattened models were found as 76.223, 136.99, and 80.791 MPa, respectively. Therefore, the hook-type model was selected as the worst case for the mechanical performance test.

**Results:** A bending test was conducted on the hook-type model without fracture and failure at 5344.56 N. The proposed customised implant was found suitable for Type IIIA acetabulum bone loss, whereas the shape suitability and mechanical safety were verified for the worst case.

**Conclusion:** The shape of a customised implant suitable for Paprosky IIIA type was designed. The shape suitability and mechanical safety were evaluated using finite element method analysis and bending tests. Clinical validation is required through subsequent clinical evaluation.

## 1. Introduction

The hip joint is a ball and socket joint. It comprises two bones: the pelvis and femur. The hip joint is susceptible to deformation, or injury because of trauma, arthritis, inflammation, etc. This can worsen without natural regeneration and cause severe pain and difficulty in walking. These hip injuries can be treated through drug therapy, osteotomy, and total hip arthroplasty (THA). Among these methods, hip arthroplasty (total hip replacement), a procedure wherein the damaged joint is replaced with various implants, has undergone significant advancements in terms of design and coating technology.<sup>1–3</sup>

In the US, approximately 100,000 THA procedures are conducted annually, which is expected to increase two-fold by 2026.<sup>4,5</sup> The initial

surgery for patients suffering from minimal damage to the pelvis is performed using a commercial cup. However, owing to subsequent implant dislocation, infection, or previous severe pelvic damage around the acetabular cup during the initial surgery, such commercial cup implants cannot be used for patients that require implant replacement. Approximately 18 out of 100 patients that underwent THA must undergo implant replacement surgery.<sup>6,7</sup>

When hip arthroplasty is performed using a commercial acetabular cup, patients suffering from large bone damage, for whom appropriate fixation on the acetabular centre is not possible, are classified as Paprosky classification Type II patients with mild migration of the hip centre.<sup>8</sup> Therefore, surgery for Type II and over patients to fill in the lost bone part is performed using a commercial implant cup with a flange,

\* Corresponding author.

\*\* Corresponding author.

E-mail addresses: [YKANG@yuhs.ac](mailto:YKANG@yuhs.ac) (J.-C. Park), [jskim@corentec.com](mailto:jskim@corentec.com) (J. Kim).

<https://doi.org/10.1016/j.jor.2022.08.011>

Received 6 April 2022; Received in revised form 29 July 2022; Accepted 7 August 2022

Available online 27 August 2022

0972-978X/© 2022 The Authors. Published by Elsevier B.V. on behalf of Professor P K Surendran Memorial Education Foundation. This is an open access article under the CC BY-NC-ND license (<http://creativecommons.org/licenses/by-nc-nd/4.0/>).

plate, and an augment. Because of this procedure, the patient may experience implant dislocation or foreign body sensation after implant replacement, owing to the mismatch with the pelvic conditions and the inserted implant cup along with the additional flange, plate, and augment. Consequently, the need for implants customised depending on the pelvic conditions of patients has increased significantly.<sup>9–13</sup>

Customised implants have gained popularity with advances in 3D printing technology. They are designed based on computed tomography (CT) data of the surgical site. This is done to ensure that they accurately fit the bones of the patients. The fabrication of customised implants using conventional methods involves time and cost issues. Therefore, 3D printing technology is considered more suitable because it can fabricate multiple products in small quantities. Moreover, 3D printing technology uses designs for additive manufacturing to fabricate implants in shapes that cannot be fabricated using conventional fabrication methods. Therefore, it has become possible to fabricate implants with porous surfaces to widen the contact surface with the bone. This increases the bonding force immediately after surgery and promotes bone growth, ensuring stable bonding of the implant.<sup>14–17</sup>

The following are the advantages of performing hip implant replacement using 3D printed customised hip implants. First, compared with other commercial products, the use of unnecessary bone resection can be avoided during surgery. This is because the bone is resected according to the defined shape of the cup and augmented when using commercial products. However, customised implants are fabricated according to the pelvis and acetabulum conditions of patients to ensure minimal bone resection. Second, customised hip implants improve surgical efficiency and shorten the operation time. Furthermore, surgical simulations can be performed by looking at the surgical site in advance with a 3D model, and the operating time and exposure to radiation can be reduced. Finally, customised implants are perfect matches for the unique anatomy of patients. Patients undergoing implant replacement already suffer severe pelvic bone damage, meaning their bone shapes are considerably different from those of healthy individuals. Therefore, by using implants fabricated according to the anatomy of such patients, the foreign body sensation that patients may experience from such implants can be reduced, whereas the stability and bonding force between the bone and implant can be increased.<sup>18,19</sup>

Therefore, in this study, we designed customised implants using CT data of a Paprosky classification Type IIIA cadaver. Furthermore, we tested the shape suitability and mechanical safety of the implants by conducting finite element analysis (FEA) and mechanical performance tests.

## 2. Materials & methods

### 2.1. Selection of implant size range according to Paprosky classification

The size range of the implant was designed according to Paprosky classification, which indicates the degree of acetabular bone loss. The implantable size range for Type IIIA cadavers and patients was set as shown in Table 1 (Fig. 1(a)). The implant total length (A), implant insertion guide hook length (C), total height (D), cup height (E), and width (G) of the implants were set to 156, 35, 105, 60, and 87 mm, respectively. Furthermore, the maximum length (B) of the flange, which enables the fixation to the pelvis, was set to 107 mm. In addition, the size range was set to apply to Type I cadavers and patients. The range of B was set to a minimum of 0 mm to exclude the flange because the fixation to the pelvis is not necessary in Type I classifications.

**Table 1**  
Implant size range.

Location	A	B	C	D	E	F	G	H	I
Normal type (mm)	44–156	0–107	0–35	24–105	24–60	0 or 5–15	44–87	0 or 17–25	0 or 8–15

### 2.2. Customised implant design based on cadaver CT data

The Mimics (Materialise N.V., Belgium) software was used to reconstruct the CT data of a Type IIIA cadaver defect bone into 3D models (Fig. 1(b)) to design customised implants (Fig. 1(c)). Based on a study,<sup>21</sup> the cup position was chosen based on the location of the pelvic acetabulum using 3matic (Materialise N.V., Belgium) software. Considering that the size of the pelvic acetabulum of the cadaver defect bone was suitable for a cup of diameter 68 mm, this cup size was applied. The basic design elements including the cup alignment, screw hole alignment, and the flange length and shape for filling the defect bone were created (Fig. 1(c)) using the above information.

As shown in Fig. 2, the design was divided based on the model type, which includes flange, hook, and flattened types. The flange was designed to bond with and support the pelvis, whereas the hook guided the location of implant placement without bonding to the pelvis.

Once the outer appearance of the model was designed, a porous structure of thickness 1 mm, pore size 550  $\mu\text{m}$ , and porosity  $\geq 60\%$  were applied to the area where the implant was in contact with the bone. This was done to increase the surface area in contact with the body and facilitate bone growth to increase the stability and grafting rate, as shown in Fig. 2(d).

The designed implant was fabricated using a powder bed fusion (PBF) type 3D printer and titanium alloy (Fig. 3).

### 2.3. Worst-case selection and testing methods for the mechanical performance test

#### 2.3.1. Selection of the worst case for the mechanical performance test

FEA was performed on the flange, hook, and flattened model types to select the worst case for the mechanical performance test. The material selected for FEA was Ti6Al4V having the following mechanical properties: density = 4405  $\text{kg/m}^3$ , elastic modulus = 107 GPa, and Poisson's ratio = 0.323. The analysis was performed by applying the same fixation conditions to all models from the tip of the ilium flange to the cup screw hole. Furthermore, additional fixed areas were applied through the ischium and pubis flange screw hole of the flange type, and the tip of the hook was fixed for the hook-type implant, as shown in Figs. 4(a) and 5 (b), respectively. For the flattened type, additional fixation conditions for both the flange and hook types were applied, as shown in Fig. 4(c).

The load applied to the implant was applied at the centre of the acetabular cup; the load generated when a 100 kg person walked on a treadmill at a speed of 7 km/h was selected from the Orthoload database (Orthoload, Germany) program according to the gait cycle. As a result, the loads applied on the anterior, medial, and superior directions were 0.73BW (715.4 N), 2.09BW (2,048.2 N), and 4.46BW (4,370.8 N), respectively. The mesh size for FEA was changed to 1 mm, and the peak von Mises stress values were compared.

#### 2.3.2. Bending test method

The MTS Bionix Tabletop Test System (MTS system, USA) was used to conduct the bending test with the hook-type specimen, which was selected as the worst case, according to three-point bending procedures. The customised implant was placed on a jig made for the test, as shown in Fig. 5. The load was applied to the centre of the cup at a rate of 5 mm/min. The test was conducted until a maximum load of 5340 N was applied or the specimen broke. A total of six specimens were repeatedly tested in accordance with ISO 7206-6 specifications.

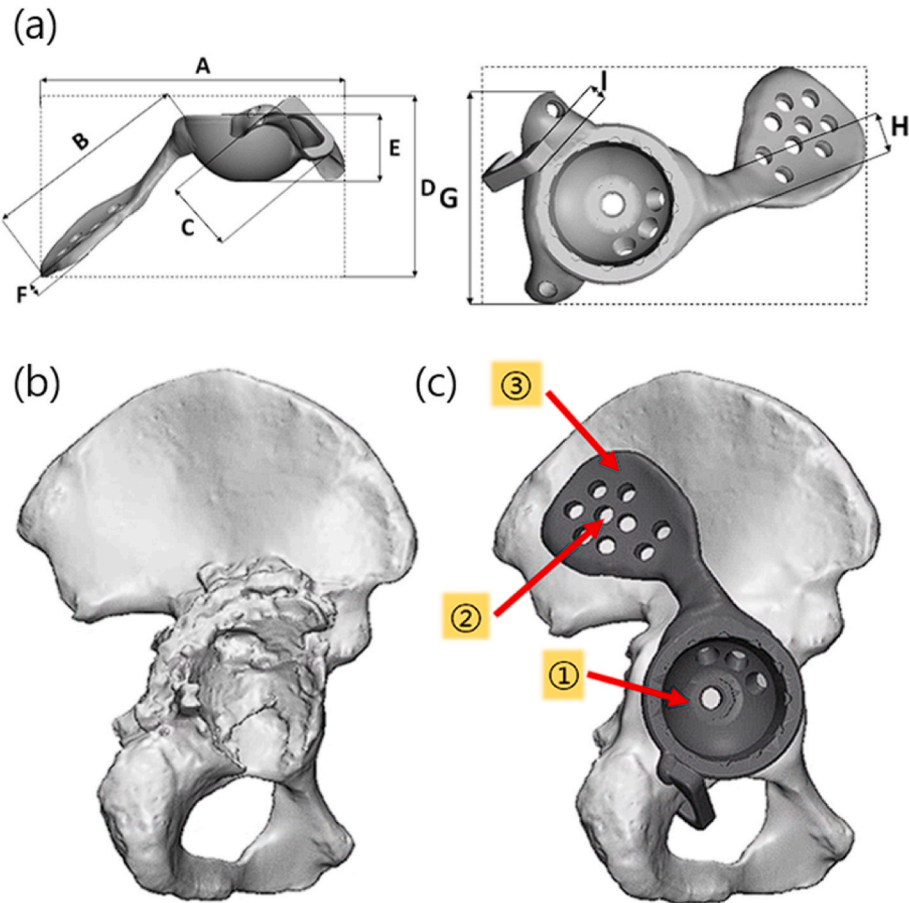


**Fig. 1.** (a) Implant design parameters, (b) Type IIIA cadaver defect bone 3D model, and (c) implantation to defect bone (1: cup alignment, 2: screw holes alignment, 3: flange length and shape).

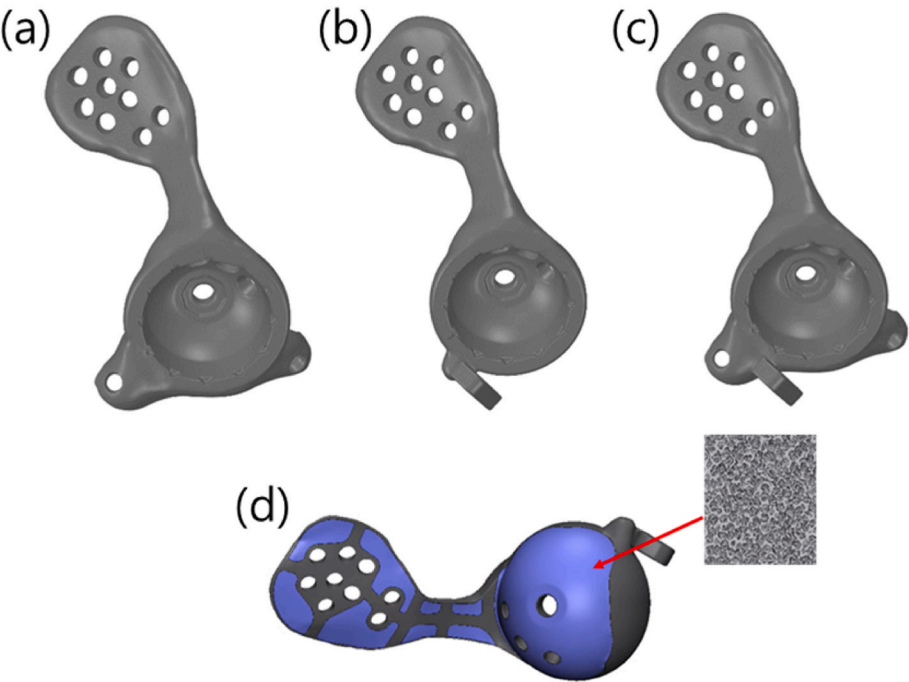


**Fig. 2.** (a) Flange type, (b) hook type, (c) flattened type, and (d) porous structure surface area.





Fig. 3. Hook type specimen produced using PBF 3D printing.

### 3. Results

#### 3.1. Analysis of the mechanical performance test results

##### 3.1.1. Worst case for the mechanical performance test

The FEA results showed peak von Mises stress values of 76.223, 136.99, and 80.791 MPa for the flange, hook, and flattened types, respectively, as shown in Fig. 6. For the worst case of the mechanical performance test, the hook type specimen exhibiting the largest peak von Mises stress was selected and used in the bending test.

##### 3.1.2. Bending test results

A bending test was conducted using Ti alloy powder and a PBF 3D printer to print the hook-type customised implant specimens for representing the worst case. Table 2 presents the bending test results. The bending test was successfully conducted up to 5344.56 N without any of the six specimens breaking. This confirmed the mechanical safety of the customised implants.

### 4. Discussion

In this study, we designed customised implants and conducted mechanical tests on the shape suitability and safety for a Paprosky

classification Type IIIA cadaver (Fig. 7). The implant specimens were fabricated using a PBF 3D printer. They were designed to have porous structures to promote bone growth and increase the fixation force. The porous structure would not be cleaned appropriately post-treatment, probably owing to the introduction of powder particles (used for 3D printing into the pores).<sup>20</sup> Therefore, it was necessary to establish a new process for cleaning customised implants with porous structures. Accordingly, more cleaning rounds with longer cleaning times as compared with those of conventional commercial methods were utilised. This was done to discharge the particles from the implants. Subsequently, a particulate detection test was conducted using a visual inspection and microscopy to verify that the cleaned implants (#1, #2, #3) would not cause problems after implantation (Fig. 8).

This study has the following limitations: first, owing to the nature of customised implants, the implant shape must be changed for each patient or cadaver according to their bone shapes. When designing a customised implant according to the bone shape of a patient, or cadaver, the most suitable acetabulum alignment similar to an existing intact bone of patient or cadaver can be achieved by following the method presented in Fig. 9<sup>21</sup>. Second, it has not been clinically validated. In this paper, the shape suitability and mechanical integrity of the customized hip implant were verified. Clinical verification will be conducted later.

The three types of customised implants proposed herein were used as the basic shapes. They were modified accordingly within the set size range to fabricate unique implants for different cadavers. Based on this

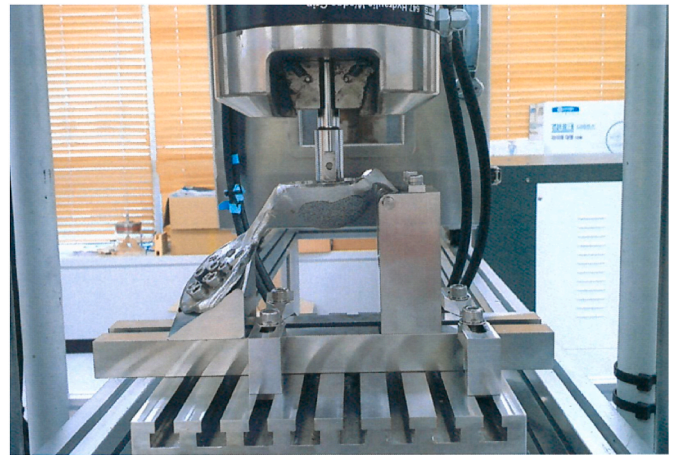


Fig. 5. Three-point bending test.

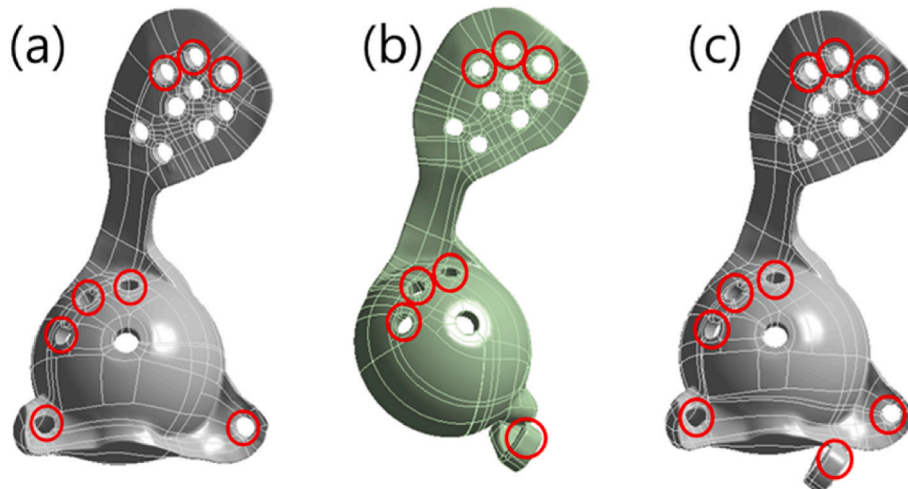


Fig. 4. Fixed area for the worst-case of different implant types: (a) Flange, (b) hook, and (c) flattened.

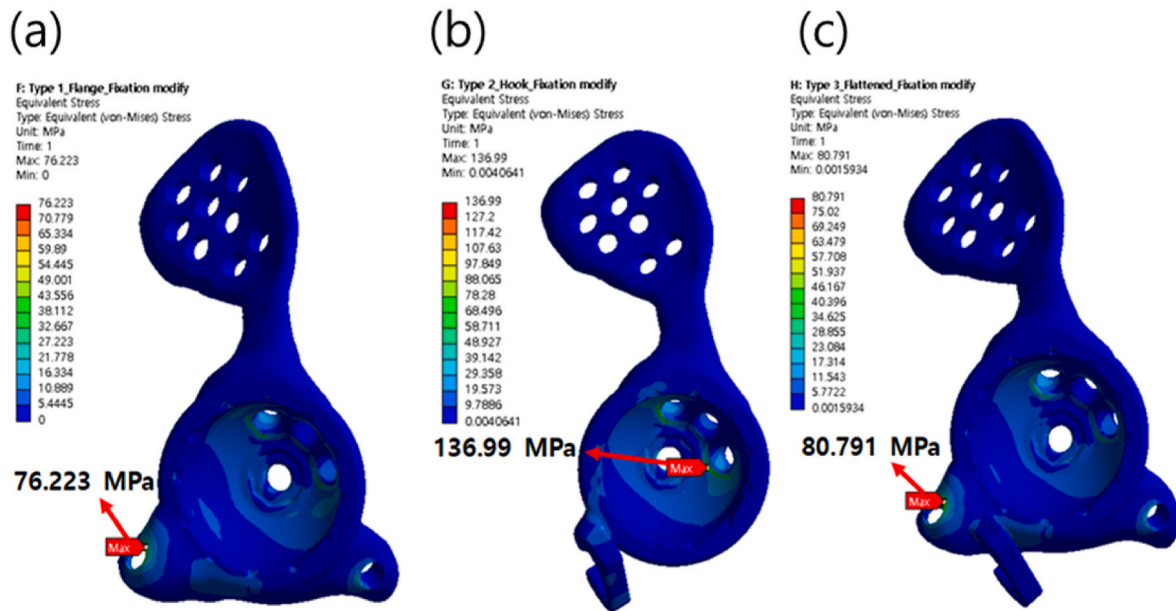


Fig. 6. FEA results of bending tests for different type implants: (a) flange, (b) hook, and (c) flattened type.

Table 2  
Bending test results.

No.	Maximum load (N)	Specimen condition
#1	5344.56 N	Not broken
#2	5343.49 N	Not broken
#3	5345.13 N	Not broken
#4	5342.22 N	Not broken
#5	5343.74 N	Not broken
#6	5340.74 N	Not broken

discussion, we designed customised hip implants suitable for a Paprosky classification Type IIIA cadaver using specific size variations. Three different types of customised hip implant model specimens, including the flange, hook, and flattened model types, were developed to assess the mechanical safety of the implants. A mechanical performance test was conducted by performing FEA to determine the worst case among the three model types. Ti alloy was used as the implant material. The load applied was set to the actual load applied to the hips of a patient weighing 100 kg when walking on a treadmill at a speed of 7 km/h. The worst-case test results showed that among the three types of customised implants, the hook-type implant was the worst because it showed the highest peak von Mises stress value of 136.99 MPa. Accordingly, the hook-type specimen was printed using Ti alloy material and a PBF 3D printer for the bending test. The bending test was conducted by applying a load of up to 5344.56 N. The results showed that none of the six specimens broke. This verified the suitability of the shape of the customised implants.

Based on the bending test results, the stress was evaluated using Equation (1). In the three-point bending test,  $g$  was 96 mm and the distance from the point where the load was applied to the hook (a vulnerable part of the stress) was 40 mm. Therefore, the load according to the distance from the point where the maximum load of the hook and flange was applied was calculated and used in Equation (1) to solve Equation (2). The results of the stress evaluation showed an average result of 212.96 MPa and confirmed the safety of the customised implant.

$$\sigma = \frac{3Fg}{2\omega d^2}, \quad (1)$$

$$\sigma = \frac{3 \times (\text{Maximum Load} \times \frac{40}{96}) \times 40}{2 \times 8.1 \times (8.8)^2}, \quad (2)$$

where  $F$  is the load applied by the texture analyser;  $\omega$  is the sample width (= 8.1 mm);  $d$  is the sample depth (= 8.8 mm); and  $g$  is the distance between supports/support gap.

Furthermore, we tested the shape suitability and mechanical safety of the customised implants for the worst-case implant (hook model type) that could be created in the Paprosky classification Type IIIA. This confirmed the need to conduct a cadaveric study or clinical trials using the tested implants. In addition, tests should be performed after the fabrication of customised implants. Additionally, a consensus should be arrived at between surgeons and patients regarding whether the shape of the implant bond is appropriate and if the patient is experiencing any foreign body sensation. Through this process, customised implants are expected to facilitate a better prognosis than the existing commercially available implants. Moreover, there is no need to remove an intact joint because customised implants are custom-made for individual patients.

A study similar to this study was conducted in 2017 at the Department of Orthopedic Surgery, Sint Maartenskliniek. In this study, a custom-made titanium material acetabular implant for 12 Paprosky Type III patients was fabricated using PBF 3D printing technology. Although the implants designed in this study are superior to clinical surgery for many patients, the mechanical safety of the flange was not evaluated.<sup>10</sup>

## 5. Conclusion

3D printing has been revolutionising the customisation of orthopaedic implant production. This can be extended to off-the-shelf implants. Printing complex porous structures and custom shapes, while achieving improved fixation with patient-specific bone morphologies, are two major advantages of 3D printing over conventional fabrication for customised implants.

Simultaneously, the importance of safety validation and standardisation of all steps involved in the production process prior to implanting into the human body was established. The International Organisation for Standardisation (ISO) and the American Society for Testing and Material (ASTM) have published guidelines related to design, materials, and testing methods.<sup>22–24</sup> However, as customised

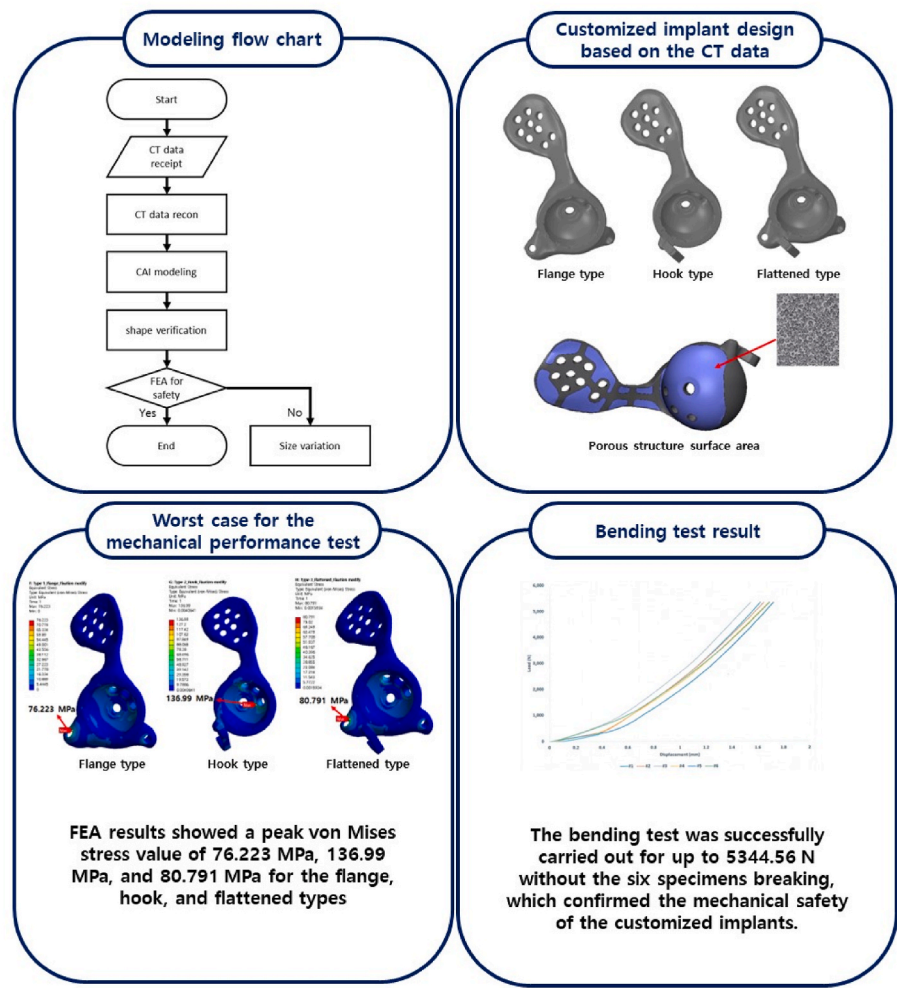


Fig. 7. Modelling flow chart, implant design, and worst-case mechanical performance and bending test results.

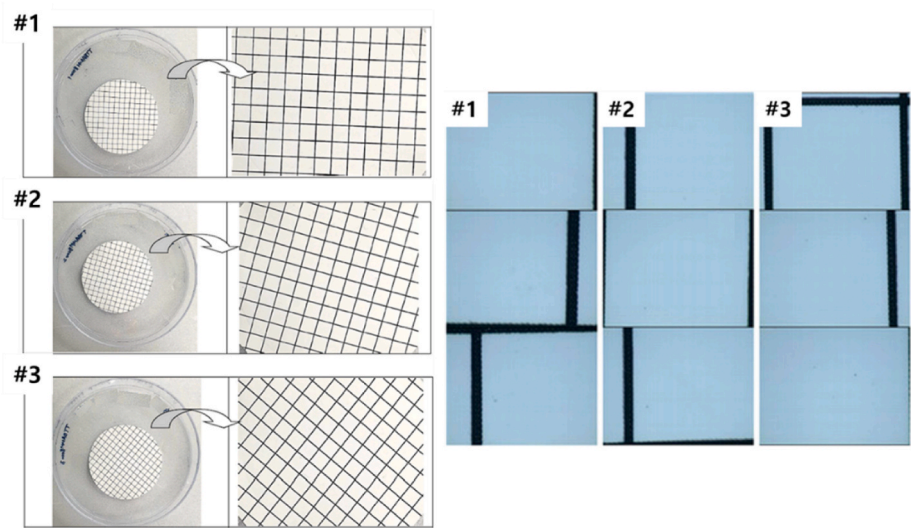
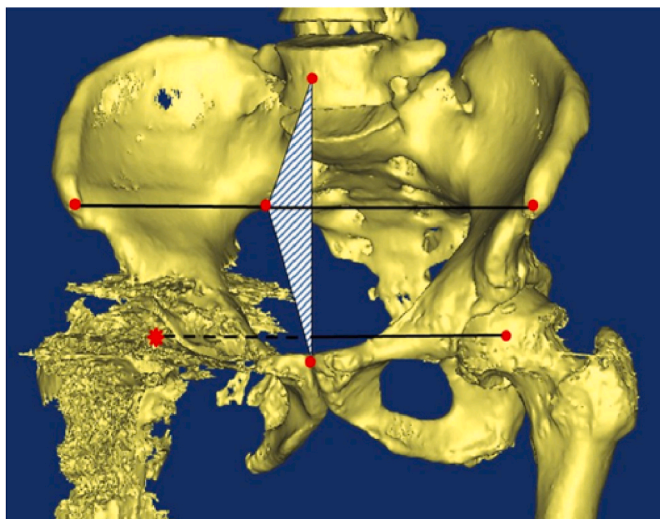


Fig. 8. (a) Particulate test results (visual inspection), and (b) particulate test results (microscopy).

implants are associated with other off-the-shelf products, 3D printing still requires significant exploration. Further investigation of various parametric characteristics of the final customised implant, to be inserted into the patient, is necessary for accommodating the potential presence

of defects.





**Fig. 9.** Method for determining the alignment of the acetabulum: 1. identify the midpoint of the line connecting the anterosuperior iliac spines and pubis symphysis, 2. identify the midpoint of the fifth lumbar vertebra, 3. create the plane, 4. mirror the alignment of the intact femoral head.

### Funding/sponsorship

This research did not receive any specific grant from funding agencies in the public, commercial, or not-for-profit sectors.

### Informed consent

Informed consent was obtained from all relevant participants included in the study.

### Institutional ethical committee approval

All the procedures performed in our study were in accordance with the ethical standards of the institutional research committee and with the 1964 Helsinki declaration and its later amendments, or comparable ethical standards.

### CRediT authorship contribution statement

Yeokyung Kang: conceptualization, methodology, investigation, software, visualization, writing—original draft, writing—review and editing.

Doo-Hoon Sun: writing—review and editing, validation, formal analysis, visualization, and supervision.

Jong-Chul Park: writing—review and editing, validation, formal analysis, resources, and project administration.

Jungsung Kim: methodology, resources, visualization, supervision, project administration, writing—review and editing.

### Declaration of competing interest

On behalf of all authors, the corresponding author states that there is no conflict of interest.

### Acknowledgements

The authors wish to acknowledge Corentec, an implant specialist company, for assistance with creating the figures included in this paper.

This research was supported by the Ministry of Trade, Industry and Energy Industrial Technology Innovation Project. (Project name: Development of 2Track Customized 3D Printing Implant Manufacturing and Commercializing Techniques for Complex Bone Fractures, 20000397).

### References

- 1 Eftekhari NS. Total hip arthroplasty. *Mosby*. 1993;1:164. -13: 978-0801616693.
- 2 Van Houcke JV, Khanduja V, Pattyn C, Audenaert E. The history of biomechanics in total hip arthroplasty. *Indian J Orthop*. 2017;51(4):359–367. <http://doi:10.4103/ortho.IJOrtho.280.17>.
- 3 Amstutz HC, ed. *Hip Arthroplasty*. New York: Churchill Livingstone; 1991. <http://doi:10.1002/jor.1100100417>.
- 4 Steiner C. HCUP Projections Report 2012–03. U.S. Agency for Healthcare Research and Quality.
- 5 Weber M, Witzmann L, Wieding J, Grifka J, Renkawitz T, Craiovan B. Customized implants for acetabular Paprosky III defects may be positioned with high accuracy in revision hip arthroplasty. *Int Orthop*. 2019;43(10):2235–2243. <http://doi:10.1007/s00264-018-4193-3>.
- 6 Alejandro Gonzalez DV. *Revision Total Hip Replacement: An Overview*. Hospital for Special Surgery; 2016.
- 7 Kim HJ, Kim JS, Han SM, You JH, Choi KW, Youn IC. Evaluation of mechanical stability in development of customized hip implant. *J Korean Soc Precis Eng*. 2009;26:31–37. eISSN 2287-8769.
- 8 Paprosky WG, Perona PG, Lawrence JM. Acetabular defect classification and surgical reconstruction in revision arthroplasty arthroplasty: a 6-year follow-up evaluation. *J Arthroplasty*. 1994;9(1):33–44. [http://doi:10.1016/0883-5403\(94\)90135-X](http://doi:10.1016/0883-5403(94)90135-X).
- 9 Telleria JJ, Gee AO. Classifications in brief: Paprosky classification of acetabular bone loss. *Clin Orthop Relat Res*. 2013;471(11):3725–3730. <http://doi:10.1007/s11999-013-3264-4>.
- 10 Baauw M, van Hellemond GG, Spruit M. A custom-made acetabular implant for Paprosky type 3 defects. *Orthopedics*. 2017;40(1):e195–e198. <http://doi:10.3928/01477447-20160902-01>.
- 11 Issack PS, Nousiainen M, Beksac B, Helfet DL, Sculco TP, Buly RL. Acetabular component revision in total hip arthroplasty. Part II: management of major bone loss and pelvic discontinuity. *Am J Orthoped*. 2009;38(11):550–556.
- 12 Scharff-Baauw M, Van Hooft ML, Van Hellemond GG, Jutte PC, Bulstra SK, Spruit M. Good results at 2-year follow-up of a custom-made triflange acetabular component for large acetabular defects and pelvic discontinuity: a prospective case series of 50 hips. *Acta Orthop*. 2021;92(3):297–303. <http://doi:10.1080/17453674.2021.1885254>.
- 13 Joshi AB, Lee J, Christensen C. Results for a custom acetabular component for acetabular deficiency. *J Arthroplasty*. 2002;17(5):643–648. <http://doi:10.1054/arth.2002.32106>.
- 14 Wyatt MC. Custom 3D-printed acetabular implants in hip surgery—innovative breakthrough or expensive bespoke upgrade? *Hip Int*. 2015;25(4):375–379. <http://doi:10.5301/hipint.5000294>.
- 15 Zanasi S, Zmerly H. Customised three-dimensional printed revision acetabular implant for large defect after failed triflange revision cup. *BMJ Case Rep*. 2020;13(5), e233965. <http://doi:10.1136/bcr-2019-233965>.
- 16 Woo SH, Sung MJ, Park KS, Yoon TR. Three-dimensional-printing technology in hip and pelvic surgery: current landscape. *Hip Pelvis*. 2020;32(1):1–10. <http://doi:10.5371/hp.2020.32.1.1>.
- 17 Park JW, Shin YC, Kang HG, Park S, Seo E, Sung H. In vivo analysis of post-joint-preserving surgery fracture of 3D-printed Ti-6Al-4V implant to treat bone cancer. *Bio-Des Manuf*. 2021;4:1–9. <http://doi:10.1007/s42242-021-00147-2>.
- 18 Hao Y, Wang L, Jiang W, et al. 3D printing hip prostheses offer accurate reconstruction, stable fixation, and functional recovery for revision total hip arthroplasty with complex acetabular bone defect. *Engineering*. 2020;6(11):1285–1290. <http://doi:10.1016/j.eng.2020.04.013>.
- 19 Di Laura A, Henckel J, Wescott R, Hothi H, Hart AJ. The effect of metal artefact on the design of custom 3D printed acetabular implants. *3D Print Med*. 2020;6(1):23. <http://doi:10.1186/s41205-020-00074-5>.
- 20 Shapovalov V. Porous metals. *MRS Bull*. 1994;19(4):24–28. <http://doi:10.1557/S0883769400039476>.
- 21 Li H, Qu X, Mao Y, Dai K, Zhu Z. Custom acetabular cages offer stable fixation and improved hip scores for revision THA with severe bone defects. *Clin Orthop Relat Res*. 2016;474(3):731–740. <http://doi:10.1007/s11999-015-4587-0>.
- 22 ISO 17296-3.. *Additive Manufacturing—General Principles Part 3: Main Characteristics and Corresponding Test Methods*. Geneva, Switzerland: International Organisation for Standardisation; 2014.
- 23 ASTM F2924-14.. *American Society for Testing and Materials (ASTM). Standard Specification for Additive Manufacturing Titanium-6 Aluminum-4 Vanadium with Powder Bed Fusion*. West Conshohocken, PA: ASTM; 2014.
- 24 ASTM 52900:2015(E). *American Society for Testing and Materials (ASTM). Standard terminology for additive manufacturing—General principles. Terminology*. West Conshohocken, PA: ASTM; 2015.